JOURNAL OF MATERIALS SCIENCE 29 (1994) 5367–5373

The influence of powder loading and binder additive on the properties of alumina injection-moulding blends

S. T. PAUL LIN
Mechanical Engineering Department, National Taiwan Institute of Technology, Taipei, Taiwan
R. M. GERMAN
Department of Engineering Science and Mechanics, The Pennsylvania State University, 118 Research West, University Park, PA 16802, USA

The effects of powder loading and binder additive on the rheology, moulding, and sintered properties of alumina injection-moulding blends were studied. The melt viscosity increased with the powder loading, which enhanced the defect concentration of the moulded parts when the powder loading was higher than 0.54 volume fraction. This transitional powder loading was much smaller than the critical powder loading of 0.65 derived by fitting the rheological data with a mathematical model. The low molecular weight acidic binder additives used in this study effectively reduced the melt viscosity. However, additives that yielded a large quantity of burn-out residue deteriorated the sintered properties. A high powder-loading mixture having a low melt viscosity and good powder dispersion was achieved by eliminating powder agglomerates before mixing, and by using an appropriate binder additive.

1. Introduction

Powder injection moulding is a fabrication process used for mass production of parts with thin walls and complex shapes [1]. Although it comprises the steps analogous to those in plastic injection moulding and other binder-assisted ceramic processes, such as slip casting and extrusion, it has unique attributes and limitations [1, 2]. Similar to other binder-assisted ceramic processes, a homogeneous and high powder packing is one of the primary goals for powder injection moulding. A homogeneous particle packing enhances sintering and reduces anisotropic shrinkage, while a high particle-packing density gives a high sintered density and smaller shrinkage vital to dimensional control. Nevertheless, a powder loading close to the critical value results in an infinitely high viscosity which retards injection moulding. Inhomogeneities in the blend for powder injection moulding arise mainly from the powder agglomerates [3, 4], poor binder wetting on the powder [5, 6], and low mechanical shearing in mixing [3, 4].

Particle dispersion is affected by the powder–binder adhesion. The surfaces of most metals, metal oxides, carbides, and nitrides are covered with polar hydrated groups. The adhesion force between the powder and binder arises from acid–base interaction [5] or covalent bonding [7–9]. Usually, a surface-active dispersant is used to bridge between the binder and powder. Dispersants based on covalent bonding are mostly organometallics. A proper organometallic dispersant reduces the flow viscosity [8, 9] and increases the green strength [9], but for incompatible powder–binder combinations there may be more difficulty in attaining a homogeneous mixture [8]. Dispersants based on acid–base reaction are mainly hydrocarbon organic materials. The acidic or basic properties of ceramic powders have been determined [10]. From the viewpoint of a Lewis acid–base interaction [5], a basic powder surface is most compatible with acidic polar binder and vice versa. An incompatible binder–powder system results in inhomogeneity of the blend and deterioration of green strength [5].

The widely used injection-moulding binders have been documented [11]. An ideal binder for powder injection moulding is a multicomponent mixture that contains a high molecular-weight backbone polymer, a low molecular-weight filler, and a flow modifier or dispersant. This combination gives good flow behaviour in injection moulding and subsequently a stepwise binder removal in debinding. The adhesion-enhancing polar binder component can be a high molecular-weight polar wax such as carnauba wax or montan wax [12], or it can be a low molecular-weight dispersant such as fish oil or stearic acid [5, 6, 10]. The low viscosity and high polarity of low molecular-weight dispersants make them more effective than the high molecular-weight waxes. A good dispersant contains a functional group that strongly anchors to the particle surface via an acid–base interaction or covalent bonding, and a carbon chain that extends into the binder [7]. These create the stabilization of the particles after they are broken apart by mechanical shearing. The dispersants are usually added to the

0022–2461

powders in a pre-treatment stage [13], whereas mixing the powder with the binder and dispersant in one batch is most desirable. This depends on the efficiency of the dispersant, and is determined by its anchoring force to the particle surface and its solubility in the binder [7]. If the dispersant is very soluble in the binder and the anchoring force to the powders is very weak, not much dispersant will stay on the particle surface and the dispersion effect is weak. On the other hand, if the anchoring force to the powders is strong and the solubility of dispersant in the binder is limited, the dispersant-coated particles can aggregate. An ideal dispersant therefore consists of an insoluble functional group that strongly anchors the dispersant to the particle surface, and a soluble chain that extends into the binder to prevent aggregation [11]. Such a good dispersant can easily reach the monolayer coverage of adsorption, or the plateau of the adsorption isotherm with a small amount of addition [10, 14].

In this work, the powder-loading effect on injection moulding was first examined. Factors limiting the use of a high powder loading were addressed. A high powder loading was then tailored by varying the binder additives using both organic and inorganic materials. Finally, the sintered properties were compared.

2. Experimental procedure

The alumina powder (A-16SG, Alcoa Inc.) had a mean particle size of 0.5 μm as determined by a laser forward light scattering method (Microtrac II). The apparent density and tap density of this powder were 27% and 33% theoretical, respectively. Doping of alumina with magnesia was compared through two routes, i.e. doping in a powder pre-treatment and doping in mixing. Some of the ionizable magnesium salts were tested as dopants, including hydrated magnesium nitrate, magnesium sulphate, and magnesium stearate. In each case, an equivalent of 0.2 mol % magnesia was added. For doping in powder pre-treatment, the powder was doped with magnesium nitrate water solution. It was followed by calcination at 400 °C, ball milling, and sieving through 170 mesh. The size of the large agglomerates after sieving was about 50 μm. Magnesium sulphate and magnesium stearate were used for doping during mixing.

The binder was a combination of low molecular-weight polypropylene, carnauba wax, paraffin wax, and a dispersant. The dispersants used in this study included stearic acid, fish oil, and phosphate ester acid (Emphos PS-21A, Witco Inc.). The amount of the dispersant for the monolayer coverage of adsorption to take place is near 3 wt % binder in most reports [7, 10, 14], and a higher concentration of dispersant is more effective [15]. After several preliminary tests, the compositions given in Table I were chosen for comparison. The binder additives were fixed at 4 wt % in binder. In blend A, the magnesia dopant was added in the powder pre-treatment as described above. Different powder loadings, ranging from 50–60 vol %, were studied for this composition. In blends B and C, stearic acid and fish oil were added as dispersants, respectively, and magnesium sulphate was added as a doping precursor during mixing. In blend D, phosphate ester acid was added as a dispersant and magnesium stearate was added as a doping agent during mixing. The powder loading was 60 vol % for blends B, C and D.

TABLE I Binder compositions for case study

	Weight fraction (%)				Density ($g\,cm^{-3}$)	Molecular weight ($g\,mol^{-1}$)
	A	B	C	D		
Polypropylene	20	20	20	20	0.90	43000
Carnauba wax	10	10	20	10	0.97	1300–1500
Paraffin wax	66	66	66	63.6	0.90	350–420
Stearic acid	4	4	0	0	0.85	285
Fish oil	0	0	4	0	0.82	–
Emphos PS-21A	0	0	0	4	1.05	100–500
Magnesium stearate	0	0	0	2.4	1.03	590

The blends were prepared with a double planetary mixer at 130 °C. The effective mixing zone of the mixer was about 7.4 litre while the combined volume of powder and binder was about 1.3 litre . The mixing time was 1 h at a maximum rotation frequency of 120 r.p.m. The binder components were added first whereas the powder was added sequentially in four batches by a time interval of 10 min. The flow behaviour of the blends was measured with a capillary rheometer. The diameter and length of the capillary were 0.1274 and 5.09 cm, respectively. The shear rate ranged from 3.51–351 s^{-1} and the temperature ranged from 110–150 °C. The moulded green specimens were prepared with a reciprocating screw-type injection-moulding machine with automatic ejection. The temperatures of the barrel and the nozzle were kept at 95 °C and the mould at 30 °C. The green rectangular bars were 5.05 cm × 1.25 cm × 0.36 cm. The binder was removed by wick-assisted thermal debinding [15, 16], conducted in air for 36 h, with 0.5 μm alumina powder as the wicking powder. The test bars were then sintered in air at a constant heating rate of 20 K min^{-1} to 1600 °C, holding for 4 h. The density of the sintered bars was measured with the water-immersion method, and the strength was measured with standard three-point bend test with a gap length of 3.2 cm. The strain rate was approximately $1.1 \times 10^{-3}\,s^{-1}$. The average strength was determined based on at least 20 specimens.

3. Results and discussion

3.1. Powder loading and rheology

Powder-filled organics often show a flow yield stress in the plot of shear stress versus shear rate [17]. The existence of a flow yield stress causes the possible separation of the binder from the binder–powder blend in extrusion, and stagnation of the blend in the region of low shear stress in mixing. Fig. 1 shows the flow curve for blend A with a powder loading of 0.56. This blend behaved as a pseudoplastic material with a flow yield stress, and was very close to a Bingham

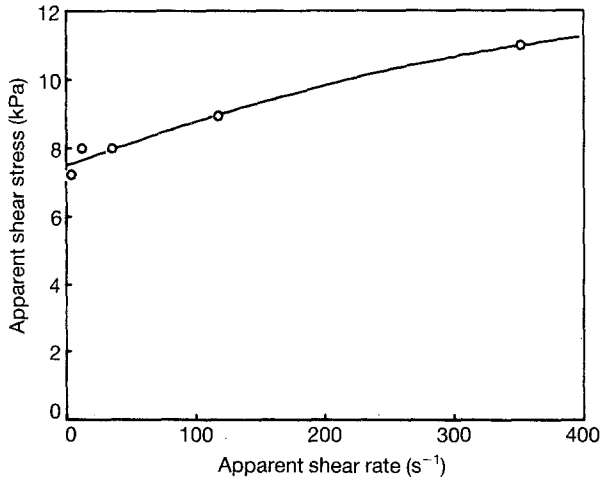

Figure 1 Flow curve for blend A having a powder loading of 0.56 volume fraction at 150 °C, showing the behaviour of a pseudoplastic body with a flow yield stress.

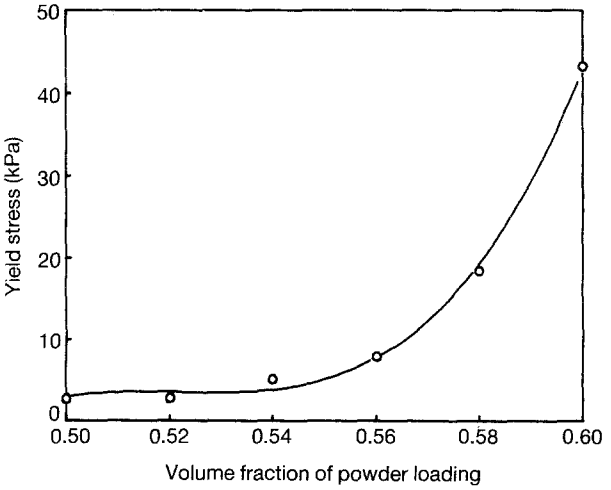

Figure 2 Variation of flow yield stress with powder loading for blend A at 150 °C.

plastic body. The value of the flow yield stress is proportional to the square of powder loading at low powder loadings [18], and increasingly deviates from the square of powder loading when the powder becomes the major component in the blend [19]. Such behaviour is shown in Fig. 2. A high flow yield stress indicates a high friction coefficient between particles, such that a high shear stress is required to start material flow. This can cause the separation of binder from the blend, if the shear stress required for the flow of binder in the porous structure is much lower than that for the flow of the blend. The separation of the binder from the blend with a powder loading of 0.6 volume fraction in capillary extrusion is shown in Fig. 3. The shear rate during extrusion changed from 3.51 s^{-1} to 351 s^{-1}. When the applied shear stress was lower than the flow yield stress of the mixture at low shear rates, the binder in the porous powder channels bore the applied pressure. The applied pressure caused binder flow in the porous channels, which in turn increased the flow yield stress of the mixture by increasing the powder loading. Therefore, a higher shear stress was required to exude the mixture. After reaching a high shear stress, the binder-depleted mixture was completely exuded out of the capillary and a low shear stress was again induced. Such behaviour was repeated in a pattern of sharp serration of the applied force.

A low mixture viscosity at a high solid content is desired for injection moulding. However, the viscosity increases dramatically once the powder loading approaches the critical value [15]. This critical value strongly depends on the binder, powder, and mixing conditions. The melt viscosity increases asymptotically with powder loading. Fig. 4 shows this phenomenon for blend A at 150 °C. Many models relating the apparent viscosity and the powder loading are available [15, 20–22]. All of these models acknowledge the substantial increase of flow viscosity with powder loading close to the critical powder loading, which has an infinite flow viscosity. However, none of these include the parameter of shear rate, although the

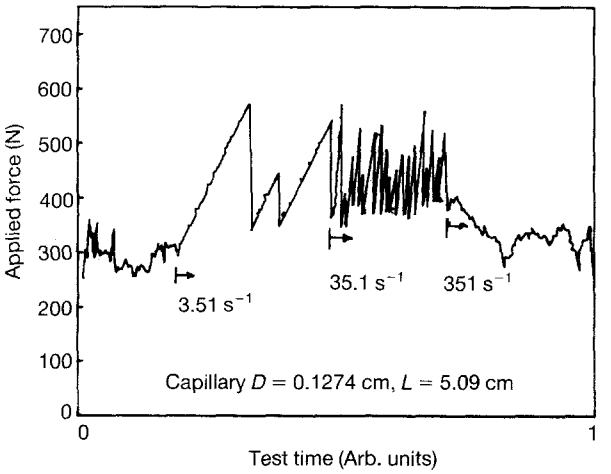

Figure 3 Capillary extrusion profile for blend A having a powder loading of 0.6 volume fraction under different shear rates at 150 °C.

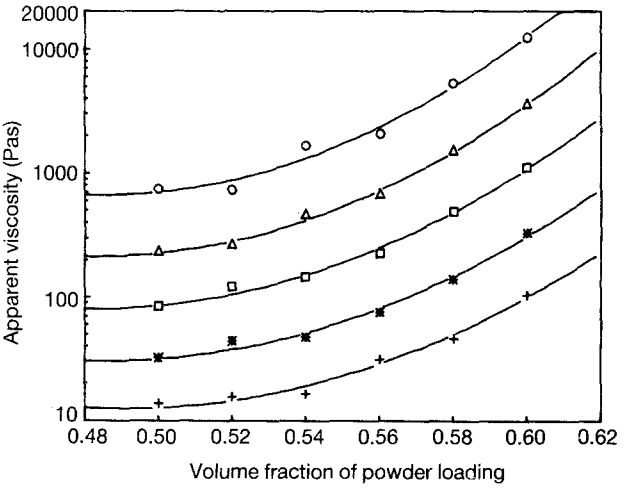

Figure 4 Flow viscosity versus powder loading at different shear rates for blend A at 150 °C: (○) 3.51 s^{-1}, (△) 11.7 s^{-1}, (□) 35.1 s^{-1}, (*) 117 s^{-1}, (+) 351 s^{-1}.

apparent viscosity is strongly dependent on the shear rate.

A particulate-filled polymer blend is a typical example of a disperse system. The viscosity of the particulate–disperse polymer blend is usually related

to the volume fraction of solid by the following equation [15]

$$\eta_r = \frac{\eta_a}{\eta_0} = \left(1 - \frac{\phi}{\phi_c}\right)^{-2} \quad (1)$$

where η_r is the reduced viscosity of the mixture, η_a the apparent viscosity of the mixture, η_0 the apparent viscosity of the binder, ϕ the volume fraction of powder loading, and ϕ_c the critical volume fraction of powder loading. The apparent viscosity is defined as the ratio of apparent shear stress, τ_a, to apparent shear rate, $\dot{\gamma}_a$

$$\eta_a = \frac{\tau_a}{\dot{\gamma}_a} = K\dot{\gamma}_a^{n-1} \quad (2)$$

where K is defined as the fluid consistency index and n is the flow behaviour index.

For a powder–binder blend exhibiting non-Newtonian flow, an apparent shear-rate dependent parameter, α, has been suggested in Equation 1 [15]

$$\eta_r = \frac{\eta_a}{\eta_0} = \alpha\left(1 - \frac{\phi}{\phi_m}\right)^{-2} \quad (3)$$

As can be seen from Fig. 1, this mixture exhibited a non-Newtonian flow behaviour. The viscosity of the pure binder was 0.2 Pa s at 150 °C. A linear regression of the viscosity data and the volume fraction of powder loading with this model yielded the following equation

$$\eta_r = \frac{\eta_a}{\eta_0} = \left(\frac{736}{\dot{\gamma}^{0.94}}\right)\left(1 - \frac{\phi}{0.65}\right)^{-2} \quad (4)$$

where $\dot{\gamma}$ was in units of s^{-1}. The critical powder loading was 0.65 volume fraction and the flow behaviour index, n, was 0.06 at 150 °C. A flow behaviour index close to zero can be characterized as having a flow pattern similar to most polymer melts [23]. For the same grade of alumina powder, a similar value of critical powder loading was obtained based on binder pyrolysis behaviour [21] and fall in mixing torque with the sequential addition of binder [24], while a much higher value (0.73–0.76) was obtained by relating viscosity to powder loading using a different empirical equation [21]. The critical powder loadings determined based on different empirical equations relating viscosity and powder loading were sometimes absurdly much higher than the highest powder loading encountered in real practice. For example, the critical powder loadings for a zirconia powder were 1.22 volume fraction and 0.70 volume fraction using different empirical equations, while the highest powder loading that could be conveniently mixed was around 0.45 [20].

3.2. Powder loading and mouldability

The effect of powder loading on the mouldability of blend A based on over 40 injection moulding trials is shown in Fig. 5 Owing to the substantial increase of flow viscosity, the moulding failure probability increased abruptly once the powder loading was higher than 0.54 volume fraction. Most of the failure specimens were associated with incomplete mould filling or visible flow lines arising from existence of pre-freezing mixture. The use of higher moulding temperatures to reduce the mixture viscosity resulted in severe cracks. The green strengths for blend A at different powder loadings are shown in Fig. 6. Also shown in this figure are the green strengths for blends B, C and D for comparison. The green strength of the powder–binder composite was higher than the strength of the pure binder (8.3 MPa), whereas a binder with a higher strength does not necessarily give a higher green strength for the moulded compact [13]. A dispersant that functions through covalent bonding to the powder increases the green strength of the powder–binder composite [9]. The green strength of the powder–binder composite increases with decreasing particle size [25]. All of these factors imply that the green strength is determined by the strength and bonding area of the particle–binder interface. For blend A, the green strength initially slowly increased with powder loading because of the increase of particle–binder interfacial bonding area per unit volume. After reaching a maximum, it then decreased substantially as the chance of entrapping voids increased with an increase in powder loading. The maximum green strength occurred at a powder loading of 0.56 volume fraction. The powder loading that yields the maximum green strength was suggested to be the critical powder loading due to the fact that the increase in mixture viscosity as a result of increasing powder loading causes more intense shearing during mixing which minimizes the chances of entrapping voids [26]. Based on this suggestion, the critical powder loading was 0.56. This value was too low compared with the other critical powder loading values (0.65–0.76) suggested by differ-

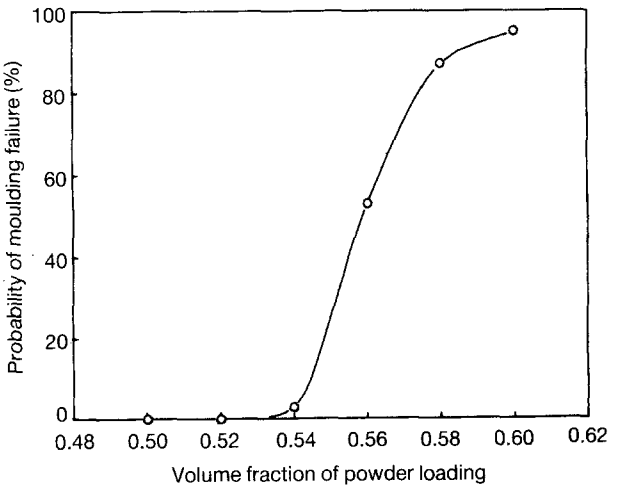

Figure 5 Probability of moulding failure versus powder loading for blend A, based on the statistics of at least 40 specimens for each powder loading.

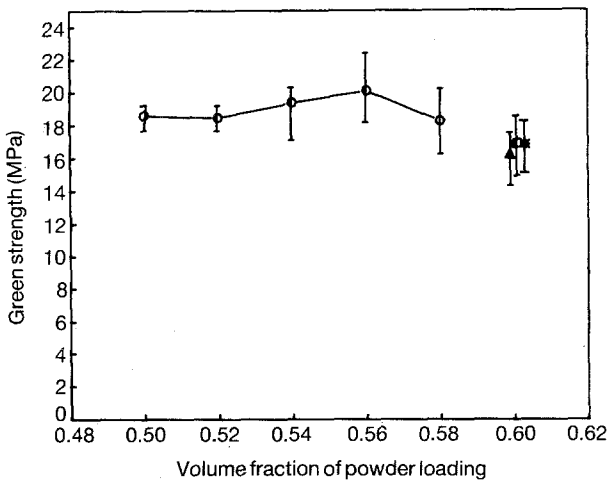

Figure 6 Green strength of the moulded parts versus volume fraction of powder loading for blends (○) A, (△) B, (□) C and (*) D.

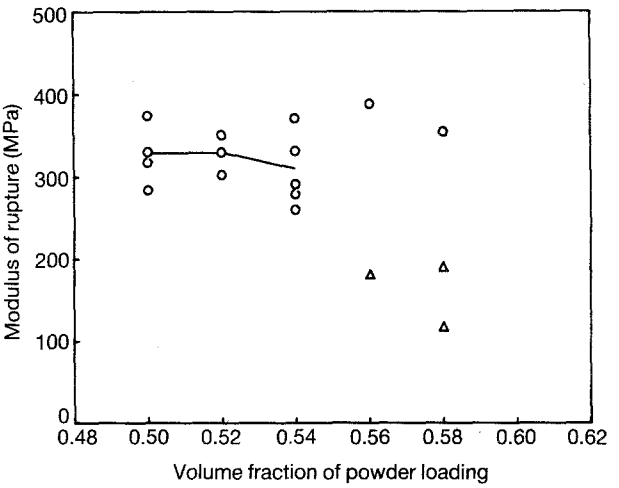

Figure 7 Modulus of rupture versus powder loading for blend A. (○) Normal failure, (△) laminated failure.

ent approaches, as shown in the previous section. A high melt viscosity that enhances flow resistance increases the mould filling time. This causes premature freezing and introduces defects in the green parts. A low viscosity at low temperatures is required for moulding parts with complex shapes. A high powder loading with suitable viscosity at low temperatures can be realized by using a low-viscosity multicomponent binder that wets the powders and still retains the desired green strength. A reduction of number and size of agglomerates can substantially enhance the powder loading. In addition, mixing at an optimum temperature [6] with a high shearing rate [3] gives better dispersion and sintered properties, while approaches such as agglomerate pre-sizing and extending the mixing time, are either tedious or apt to cause property changes in the binder [27] or introduces impurities [28].

The cause of defects due to a high flow viscosity was more evident after sintering. Both normal and laminated failures were observed for parts moulded with a high powder loading. The laminated failure mode gives very low strengths. Fig. 7 shows the sintered strength for different powder loadings. The scatter in sintered strength increased with the increase of powder loading. The optimum powder loading for blend A was 0.54 volume fraction while its theoretical maximum powder loading was 0.65 volume fraction as indicated in Equation 4. It is therefore very clear that a compromise must be made between sintering shrinkage and moulding defects arising from the variations of powder loading.

3.3. Dispersant and rheology

Most of the commercially available dispersants lie in the category of semisteric stabilization because of their low molecular weight [5]. Fig. 8 shows the effect of different dispersants on the melt viscosity at 60 vol % solid and 150 °C. For blend A, the extrusion flow pattern showed sharp serrations in the force–time plot (Fig. 3). This indicated inhomogeneity due to the existence of hard agglomerates (possibly arising from

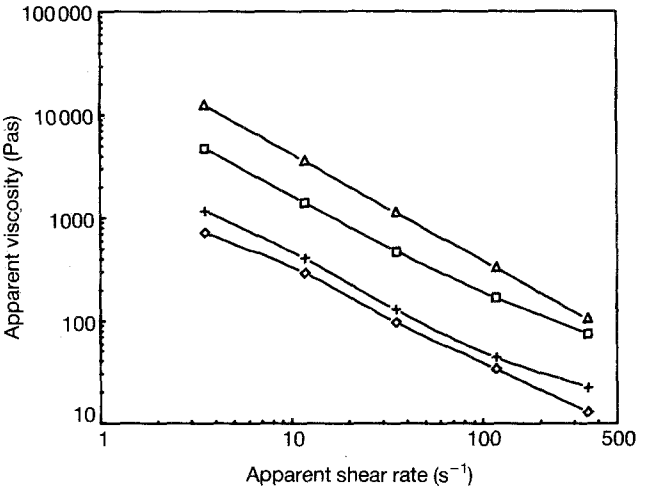

Figure 8 The effect of dispersant on the flow behaviour of blends (△) A, (+) B, (□) C and (◇) D, having 60 vol % powder loading at 150 °C.

calcination at 400 °C) that were not broken apart by the low mechanical shearing during mixing. The resistance to flow could be substantially reduced when the powder calcination step was avoided, as indicated by the flow behaviour of blend B. Stearic acid effectively reduces the flow viscosity of the injection-moulding blend [15, 16]. The addition of 1 wt % stearic acid reduces the flow viscosity of pure binder by about 8% [15], and the flow viscosity of carbonyl iron powder mixture by about 20% [29]. The addition of stearic acid to the powder as a powder pre-coating prior to mixing gives better mixing homogeneity than the addition of stearic acid to the powder during mixing [13]. Additionally, the green strength is not substantially changed with the addition of stearic acid [29]. Therefore, stearic acid is not a very efficient adhesion-enhancing dispersant, but a good flow modifier. Fish oil has been widely used in both tape-casting [10, 14] and injection-moulding processes [30] to improve the dispersion of fine ceramic powders in organic binders. Nevertheless, its effect was reported to be less than the derivatives of fatty acids such as oleic acid and stearic acid [31] while the contrary

observation was also reported [7]. In contrast to stearic acid, fish oil was not very effective in reducing the flow viscosity of the powder–binder blend as indicated by comparing the flow behaviour of blends B and C. Emphos PS-21A, a phosphate ester acid, is a strong acidic-type dispersant with a pH value of about 2. Out of 29 dispersants tested, this phosphate ester acid was reported to affect the dispersion and flow viscosity of the powder–binder blend most effectively in tape casting [10]. Magnesium stearate, a popular lubricant and mould-release agent, can be a candidate for serving as a lubricant and magnesia-doping precursor. This combination gave a significant reduction on flow viscosity compared with the other additives tested.

The effect of temperature on the melt viscosity followed an Arrhenius equation in a single-component binder system [3, 15]. For the multicomponent binder system used in this study, the temperature dependence of melt viscosity was roughly divided into two regions. Fig. 9 shows this behaviour for blend A having a powder loading of 0.56 volume fraction. As temperature increased, the flow viscosity decreased and reached a close-to-constant value when the temperature was higher than the melting temperature of polypropylene (147 °C, prior to mixing). The activation energies for flow were 140 and 3.1 kJ mol^{-1} for the low-temperature and high-temperature regions, respectively. The typical activation energy for successful injection moulding lies in the range between 14 and 18 kJ mol^{-1} [15, 32], while a much lower activation energy is the main requirement for low-pressure injection moulding [3]. The high activation energy encountered due to cooling resulted in escalation of viscosity, and caused stress concentration, cracking, and distortion in the moulded parts. Injection moulding is expected to be very sensitive to the injection pressure and speed when it is carried out at temperatures whose activation energy for flow is high. However, barrel temperatures around 95 °C were found to optimal for injection moulding without having visible defects in the green parts in this study. A higher temperature (> 120 °C) caused shrinkage cracks near the end of the die cavity. A lower temperature (85 °C) caused difficulty in die filling due to a high flow viscosity.

3.4. Sintered properties

The average sintered densities were 98.5%, 98.6%, 98.4% and 92.9% theoretical for blends A–D, respectively. The low sintered density for blend D was caused by the existence of binder burn-out residues of magnesium stearate and phosphate ester acid. Fig. 10 shows the decomposition profiles of these two materials as well as stearic acid in air. The residual carbon inhibits final sintering of alumina by reacting with alumina and forming vaporizing aluminium suboxides and carbon oxides at temperatures at which final-stage sintering of alumina takes place [33]. For most inorganic dispersants, carbides are very common residues after binder burn-out [8]. Therefore, this group of dispersants are not suitable for this powder, especially when their clean burn-out temperatures are higher than the sintering densification temperature of powders.

The average flexural strengths for blends A–D were 320 MPa, 372 MPa, 355 MPa and 266 MPa, respectively. The average flexural strength for blend A was the average value for specimens having normal failure, ignoring those specimens that delaminated during testing. Blend A had a lower average strength than blends B and C even though they had approximately the same average density. The existence of hard agglomerates due to powder calcination and the higher number of moulding defects due to higher flow viscosity were the causes of lower strength. In contrast to blend A, blends B and C did not experience the calcination due to the use of magnesium sulphate as a doping agent. Avoidance of the formation of new agglomerates resulted in higher strengths. Blend D had the lowest strength because of the lowest sintered density. For blend B, the average strength was 372 MPa, which was comparable to those obtained

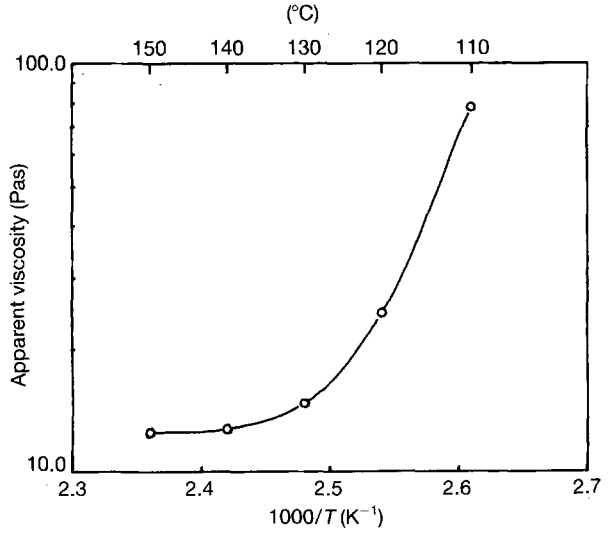

Figure 9 The temperature dependence of flow viscosity at a shear rate of 351 s^{-1} and powder loading of 60 vol % for blend A.

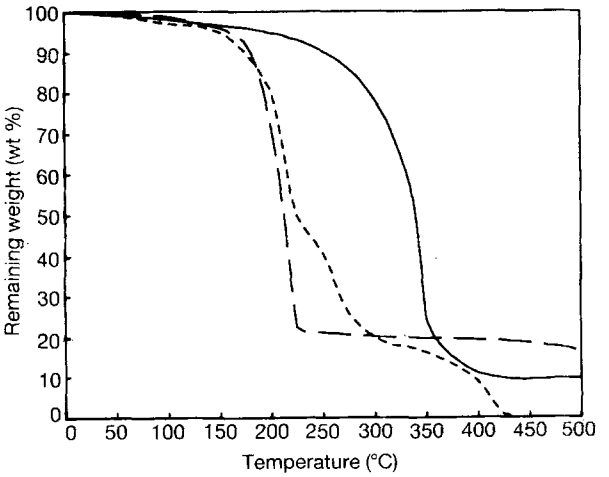

Figure 10 Decomposition profiles of (———) magnesium stearate, (— —) phosphate ester acid, and (– – –) stearic acid in air, tested under a ramp of 10 K min^{-1}.

through press and sinter [34], and injection moulding [3, 35].

4. Conclusion

A non-hydrated magnesium salt is suitable for doping alumina during mixing. This avoids the formation of new hard agglomerates. Powder loading determines the flow viscosity of the powder–binder blend and, therefore, the moulding defects. Stearic acid is a more efficient flow modifier than fish oil. It also gives a clean burn-out compared with phosphate ester acid and magnesium stearate, and is suitable for a powder whose sintered properties are deteriorated by carbide residues.

References

1. R. M. GERMAN, "Powder Injection Molding" (Metal Powder Industries Federation, Princeton, NJ, 1990) p. 1.
2. A. KATO, S. NAKAMURA, T. KAWASHIMA and H. NISHIO, *NKK Tech. Rev.* **57** (1988) 33.
3. K. MIYAMOTO, Y. TAKAHASHI, S. INAMURA and H. MIYAMOTO, *J. Jpn Soc. Powder Powder Metall.* **34** (1987) 12.
4. K. N. HUNT and J. R. G. EVANS, *Trans. J. Br. Ceram. Soc.* **87** (1988) 17.
5. F. M. FOWKES, in "Ceramic Powder Science", edited by G. L. Messing, K. S. Mazdiyasni, J. W. McCauley and R. A. Haber (American Ceramic Society, Westerville, OH, 1987) p. 411.
6. M. D. SACKS, C. S. KHADILKAR, G. W. SCHEIFFELE, A. V. SHENOY, J. H. DOW and R. S. SHEU, *ibid.* p. 495.
7. M. GREEN, T. KRAMER, M. PARISH, J. FOX, R. LALANANDHAM, W. RHINE, S. BARCLAY, P. CALVERT and H. K. BOWEN, *ibid.* p. 449.
8. K. LINDQVIST, E. CARLSTROM, M. PERSSON and R. CARLSSON, *J. Am. Ceram. Soc.* **72** (1989) 99.
9. J. G. ZHANG, M. J. EDIRISINGHE and J. R. G. EVANS, *J. Mater. Sci.* **23** (1988) 2115.
10. K. MIKESKA and W. R. CANNON, in "Forming of Ceramics", edited by J. A. Mangels and G. L. Messing (American Ceramic Society, Westerville, OH, 1984) p. 164.
11. R. M. GERMAN, K. F. HENS and S. T. PAUL LIN, *Bull. Am. Ceram. Soc.* **70** (1991) 1294.
12. M. T. MARTYN, P. J. JAMES and B. HAWORTH, *Metal Powder Rep.* **43** (1988) 816.
13. C. I. CHUNG, B. O. RHEE, M. Y. CAO and C. X. LIU, in "Advances in Powder Metallurgy", Vol. 3, edited by T. G. Gasbarre and W. F. Jandeska (Metal Powder Industries Federation, Princeton, NJ, 1989) p. 67.
14. V. L. RICHARDS II, *J. Am. Ceram. Soc.* **72** (1989) 325.
15. B. J. CARPENTER, MS thesis, Rensselaer Polytechnic Institute, Troy, NY (1988).
16. R. M. GERMAN, *Int. J. Powder Met.* **23** (1987) 237.
17. M. J. EDIRISINGHE and J. R. G. EVANS, *J. Mater. Sci.* **22** (1987) 269.
18. W. B. RUSSEL, *J. Rheol.* **24** (1980) 287.
19. J. W. GOODWIN, *Bull. Am. Ceram. Soc.* **69** (1990) 1694.
20. K. N. HUNT, J. R. G. EVANS and J. WOODTHORPE, *Trans. J. Br. Ceram. Soc.* **87** (1988) 17.
21. J. K. WRIGHT, M. J. EDIRISINGHE, J. G. ZHANG and J. R. G. EVANS, *J. Am. Ceram. Soc.* **73** (1990) 2653.
22. J. A. MANGELS and R. M. WILLIAMS, *Bull. Am. Ceram. Soc.* **62** (1983) 601.
23. D. J. WILLIAM, in "Polymer Science and Engineering", (Englewood Cliffs, NJ 1972) p. 352.
24. C. F. MAEKHOFFF, B. C. MUTSUDDY and J. W. LEMMON, in "Forming of Ceramics", edited by J. A. Mangels and G. L. Messing (American Ceramic Society, Westerville, OH, 1984) p. 346.
25. Y. SUETSUGU and J. L. WHITE, *J. Appl. Polym. Sci.* **28** (1983) 1481.
26. U. K. PUJARI, *J. Am. Ceram. Soc.* **72** (1989) 1981.
27. M. TAKAHASHI, S. SUZUKI, H. NITANADA and Z. ARAI, *ibid.* **71** (1988) 1093.
28. S. T. LIN, PhD thesis, Rensselaer Polytechnic Institute, Troy, NY, January 1991.
29. K. F. HENS, S. T. LIN, R. M. GERMAN and D. LEE, *J. Metals* **41** (1989) 17.
30. B. C. MUTSUDDY, *Adv. Ceram. Mater.* **2** (1987) 213.
31. R. E. JOHNSON Jr and W. H. MORRISON Jr, in "Ceramic Powder Science", edited by G. L. Messing, K. S. Mazdiyasni, J. W. McCauley and R. A. Haber (American Ceramic Society, Westerville, OH, 1987) p. 323.
32. P. H. BOOKER, presented at the Powder Injection Molding International Symposium, Albany, NY, July 1991 (Metal Powder Industries Federation, Princetown, NY).
33. F. J. KLUNG, W. D. PASCO and M. P. BOROM, *J. Am. Ceram. Soc.* **65** (1982) 619.
34. R. W. DAVIDGE, "Mechanical Behavior of Ceramics" (Cambridge University Press, Cambridge, 1979) p. 146.
35. B. C. MUTSUDDY, *Powder Met. Int.* **19** (1987) 43.

Received 23 August 1993
and accepted 22 April 1994